

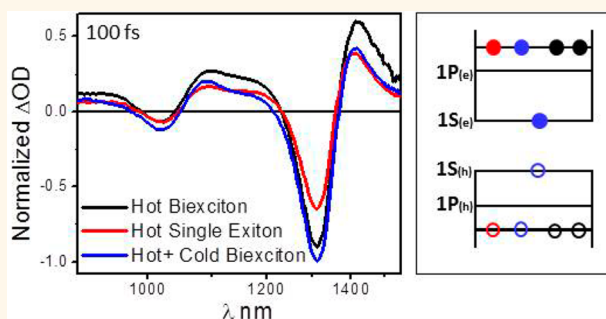
# Three-Pulse Femtosecond Spectroscopy of PbSe Nanocrystals: 1S Bleach Nonlinearity and Sub-Band-Edge Excited-State Absorption Assignment

Itay Gdor,<sup>†</sup> Arthur Shapiro,<sup>‡</sup> Chunfan Yang,<sup>†</sup> Diana Yanover,<sup>‡</sup> Efrat Lifshitz,<sup>\*,‡</sup> and Sanford Ruhman<sup>\*,†</sup>

<sup>†</sup>Institute of Chemistry, The Hebrew University, Jerusalem 91904, Israel and <sup>‡</sup>Department of Chemistry and Solid State Institute, Technion, Haifa 32000, Israel

**ABSTRACT** Above band-edge photoexcitation of PbSe nanocrystals induces strong below band gap absorption as well as a multiphased buildup of bleaching in the  $1S_e1S_h$  transition. The amplitudes and kinetics of these features deviate from expectations based on biexciton shifts and state filling, which are the mechanisms usually evoked to explain them. To clarify these discrepancies, the same transitions are investigated here by double-pump–probe spectroscopy. Re-exciting in the below band gap induced absorption characteristic of hot excitons is shown to produce additional excitons with high probability. In addition,

pump–probe experiments on a sample saturated with single relaxed excitons prove that the resulting  $1S_e1S_h$  bleach is not linear with the number of excitons per nanocrystal. This finding holds for two samples differing significantly in size, demonstrating its generality. Analysis of the results suggests that below band edge induced absorption in hot exciton states is due to excited-state absorption and not to shifted absorption of cold carriers and that  $1S_e1S_h$  bleach signals are not an accurate counter of sample excitons when their distribution includes multiexciton states.



**KEYWORDS:** quantum dots · nanocrystals · multiexciton generation · ultrafast spectroscopy · exciton cooling

Many unique qualities of semiconductor quantum dots arise from the fact that their volume is smaller than that of a relaxed exciton in the bulk solid. An important consequence of this quantum confinement is an enhancement of Coulomb interaction effects between photoinduced charge carriers due to the forced overlap of their electronic wave functions.<sup>1,2</sup> This in turn has a number of important spectral and dynamical implications, including a progressive red shifting of the discrete near band edge absorption bands with the number of existing excitons<sup>3</sup> and a marked increase in the rates of hot exciton relaxation or cooling.<sup>4,5</sup> Specifically, Auger-type e–h energy transfer mediated by Coulomb coupling becomes an efficient channel for electron intraband relaxation, which can overshadow phonon-assisted relaxation mechanisms.<sup>6,7</sup> Furthermore, strong

carrier–carrier interactions lead to the fast decay of multiexcitons via nonradiative Auger recombination in which the e–h recombination does not produce a photon but instead releases the excess as kinetic energy to a third carrier in the nanocrystals (NCs).<sup>8,9</sup>

Ultrafast transient absorption (TA) is an important experimental tool for following exciton cooling and measuring multiexciton interactions. By monitoring absorption changes ( $\Delta OD(\lambda, t)$ ) in the time and spectral domains, information on the processes described above is obtained in real time. The interpretation of TA signals from quantum dot (QD) samples has been based on two main effects: state filling and biexciton interactions.<sup>10,11</sup> The former derives from the Pauli exclusion principle, where filling of electronic states leads to blocking of the corresponding optical transitions. This phenomenon affects only transitions that

\* Address correspondence to efrat333@gmail.com, sandy@mail.huji.ac.il.

Received for review December 31, 2014 and accepted January 28, 2015.

Published online January 28, 2015  
10.1021/nn5074868

© 2015 American Chemical Society

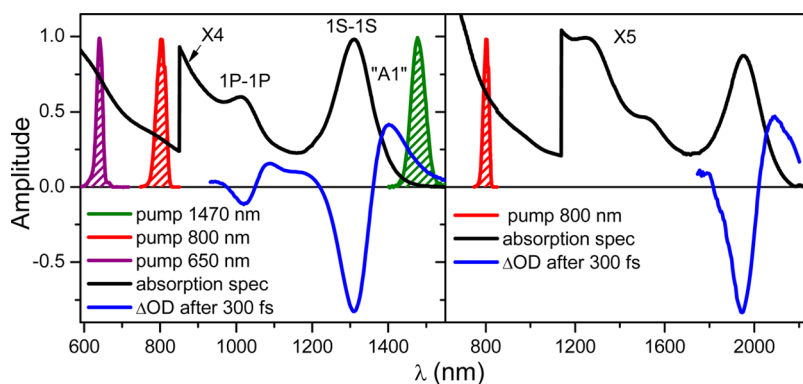


**Figure 1.** Steady-state absorption and excitation pulse spectra for 3.5 nm (left panel) and 7 nm (right panel) PbSe nanocrystals.  $\Delta$ OD spectra at a delay of 300 fs after excitation at 640 and 800 nm of the former and latter samples, respectively, are presented as well (see also Figure 2).

involve occupied states, and its contribution to  $\Delta$ OD is determined by the occupation factors of the quantized levels. Therefore, state-filling-induced TA signals are used to quantify exciton populations in QDs and to derive average exciton numbers per quantum dot.<sup>12</sup>

Biexciton interactions lead to modifications in level energies and to frequency shifts in related optical transitions.<sup>13,14</sup> Biexciton Coulomb interactions may also partially allow forbidden transitions by perturbing the electronic states.<sup>15,16</sup> In the context of TA spectroscopy, biexciton shifts involve interactions of  $e-h$  pairs excited by the pump pulse with an additional exciton generated by the probe. According to this picture, above band gap (BG) excitation should not alter the occupancy of the HOMO or LUMO; therefore immediately after excitation any changes in absorption spectrum near the band edge (BE) should stem only from biexciton shifts, which when attractive will induce enhanced absorption to the red of the  $1S_e1S_h$  band (abbreviated as 1S hereafter). Experiments focusing mainly on CdSe QDs showed that following a rapid initial appearance the band edge bleach signal continues to rise gradually over a period of several picoseconds.<sup>14</sup> This delayed rise was attributed to exciton cooling to the band edge and a switch from biexciton shifting to state filling.<sup>17</sup> These two mechanisms have also served in analyzing TA experiments on PbSe nanocrystals.<sup>18,19</sup> However, in previous high time resolution TA studies of PbSe from this lab<sup>20,21</sup> several fundamental inconsistencies with this picture were detected:

(1) Instead of a delayed rise of 1S bleach, accompanied by spectral shifting to the red following above band edge photoexcitation, in accordance with a dynamic change from biexciton shifting to state filling, the bleach buildup was nearly immediate with no delayed shift in frequency.

(2) Despite this immediate rise, simultaneous appearance of induced absorptions surrounding it leads to a net enhancement in transition dipole strength of the sample across the probed range (900 to 1700 nm), contrary to predictions from biexciton shifts and state

filling, which should either not affect the dipole strength or reduce it, respectively.

(3) Detailed analysis of the first several picoseconds of spectral evolution after pumping above the BE show that the transient absorption to the red of the BE associated with a shifted 1S transition (A1 band)<sup>12</sup> decays without a matching appearance of absorption, questioning its origin as one-half of a biexciton shift feature. Additional spectral structures were also detected in the transient absorption during cooling, which evolved on different time scales, possibly reflecting different relaxation mechanisms.

The objective of this study is to utilize more intricate TA experiments, based on double-pump-pulse schemes, directed at highly monodisperse QD samples, in order to analyze those features and identify the underlying mechanisms. Through these experiments a better understanding of the cooling dynamics of “hot” single and multiexcitons in colloidal PbSe QDs is sought. As shown below, the results are inconsistent with a number of accepted paradigms of TA in QDs and call for revisions not only in our view of exciton cooling dynamics in nanocrystals but also in the interpretation of TA data that reflect them.

## RESULTS

**Absorption and Conventional Pump-Probe.** The steady-state absorption spectrum of the 3.5 and 7 nm diameter PbSe QDs along with intensity spectra of the excitation pulses centered at 650, 800, and 1470 nm are presented in Figure 1. The prominent band edge absorption feature, centered at 1310 and 1950 nm for 3.5 and 7 nm samples, respectively, is the 1S band described above. The second is assigned to an exciton with both electron and hole having 1P envelope functions and is abbreviated 1P.<sup>22,23</sup> We note that, while prevalent, this assignment is not unanimously accepted.<sup>24</sup> At shorter wavelengths, faint additional spectral features associated with higher transitions are observable for both samples superimposed on a steeply rising absorptive background.<sup>25</sup>

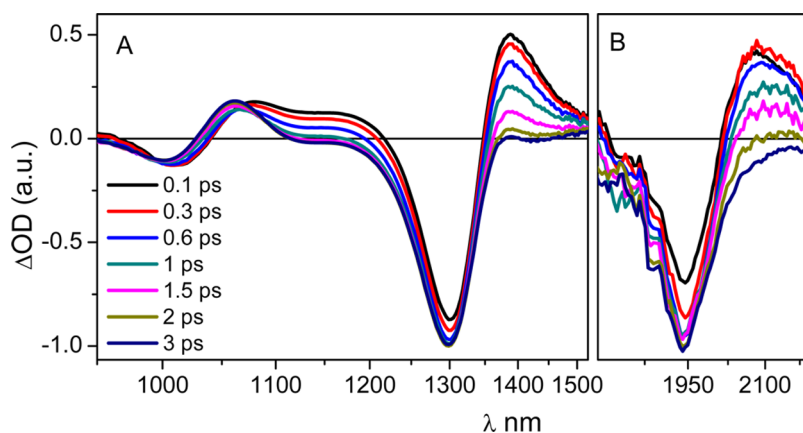


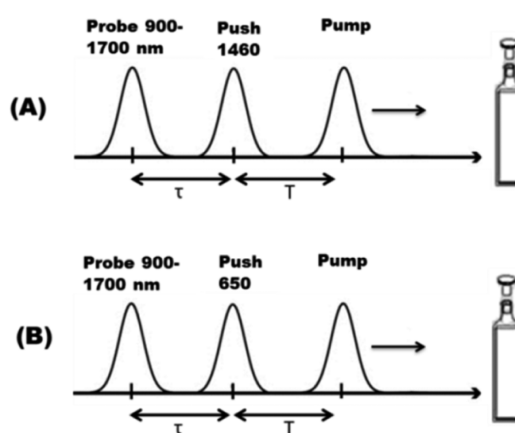
Figure 2. Transient difference spectra covering the process of exciton cooling of the 3.5 nm particle following 640 nm excitation (A) and of the 7 nm particles following 800 nm excitation (B).

A progression of transient NIR absorption spectra collected from a suspension of 3.5 nm diameter crystals, illustrating the process of exciton cooling, are presented in panel A of Figure 2. Upon 640 nm photoexcitation, intense bleaching of the 1S band appears. Near the 1P transition the excitation gives rise immediately to a superposition of bleach and red shift, which converge within picoseconds to a biexciton shifting band shape known to characterize the difference spectrum after cooling.<sup>23</sup> Along with these localized spectral changes, a broad absorption that extends to wavelengths above that of the band edge also appears promptly.

Over the course of exciton cooling, portions of the induced absorption surrounding the 1S bleach decay on different time scales, demonstrating that it consists of separate distinct bands. This fading goes on with nearly no change in position or depth of the band edge bleach, which persists along with the 1P biexciton shift feature. As demonstrated quantitatively by the measures introduced in earlier studies,<sup>20,21</sup> examination of the spectra in panel A of Figure 2 shows the relative longevity of the intense red induced absorption designated in Figure 1 as “A1”. They also demonstrate the absence of a matching change in the band edge bleach discussed in the introduction.

Particles of 7 nm diameter were studied to test the generality of findings in the smaller sample and to test for size dependence of the observed relaxation rates. For the larger sized particles probing is limited to the 1S band and its immediate surroundings, covering most of the A1 peak as well. Pumping at 800 nm produces equivalent spectral evolution as displayed in panel B of Figure 2. Rates of the processes reflected in the two sequences show significant size dependence, which will be discussed later.

Double pump–probe spectroscopy is applied here in order to understand departures from the expected spectral behavior reported previously. This method has proven very effective in identifying absorbing or



Scheme 1. (A) The push is aimed at re-exciting the sample in the transient A1 induced absorption. (B) The push excites the sample high above band edge, dosing it with additional excitons in a range that is unaffected by pre-existing excitations.

emitting intermediate states in ultrafast studies of molecular systems.<sup>26–28</sup> The idea is to test the response of a short-lived excited intermediate to secondary photoexcitation at particular delays after the initiating pump pulse. The response serves to identify the intermediate and provide constraints for building reliable dynamic schemes for the reactions under study. Two versions employed here are depicted in Scheme 1. The first involves transient re-excitation in the “A1” band of hot exciton states, while the second entails re-excitation high above the band edge of nanocrystals each of which already contains a cold “spectator” exciton.

**800 nm Pump–1470 nm Push Spectroscopy of a 3.5 nm Sample.** The opportunity to conduct this experiment is demonstrated in Figure 1, panel A. Comparing the steady-state absorption with transient transmission changes of a hot exciton shows the sudden rise in pump-induced absorption just below the BG, where nearly none existed before. The aim is to generate a hot exciton population and then re-excite directly into the

induced red absorption. The sample was thus excited at time zero with an intense ( $\eta_0(\lambda_{800\text{ nm}}) = 1.5$ )  $\sim 30$  fs pulse at 800 nm and 300 fs later irradiated with a weaker pulse at 1470 nm of similar duration.

Given the significant spectral width of the secondary pump or “push” and the inherent size distribution of the QDs, some are directly excited by the push pulse, even without prior excitation. Hence, before implementing the three-pulse experiment, simple pump–probe measurements exciting at 1470 nm were conducted. This gives rise directly to a transient difference spectrum characteristic of cold exciton states, as shown in Figure 3. Closer inspection however shows that direct 1470 nm excitation leads to spectral features that are sharper (1S bleach fwhm is reduced from 90 nm/80 meV to 75 nm/60 meV) and red-shifted by 20 nm/15 meV relative to above band edge excitation. This is assigned to population selection in the sample; the deep NIR pump energy is absorbed preferentially by larger particles whose absorption extends to lower photon energies. This selection generates a narrower size distribution of low band edge excited dots, leading to the observed trends in analogy with similar effects previously observed in

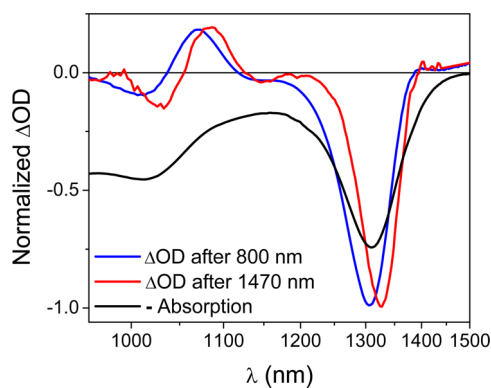


**Figure 3.** Transient difference spectra at 3 ps pump–probe delays, after excitation at 800 nm (blue line) and 1470 nm (red line) compared to the absorption spectra (black line).

fluorescence.<sup>29,30</sup> Due to the room-temperature conditions and the spectral breadth of the ultrafast excitation pulses employed, these narrowing effects are not on par with those observed in fluorescence.

The results of the double-pump–probe experiments on 3.5 nm QDs for  $\tau = 1$  ps and various values of  $T$  times are presented in Figure 4, along with the regular pump–probe experiment described above for comparison. The optical chopping is performed on the push (1470 nm) beam, meaning that the spectra demonstrate transmission changes solely due to the “push”. When it arrives before the excess photon energy is dissipated and the induced A1 absorption is at its peak ( $T = 300$  fs, black line), an increase in the band edge bleach amplitude is observed after an additional 1 ps  $\tau$  delay. This indicates that pre-exciting the sample with 800 nm irradiation increases the effectiveness of the push to be absorbed and that the extra photons absorbed by the already excited particle (transition to XX level using Kambhampati notation),<sup>31</sup> at least in part, generate additional excitons. In contrast, for  $T = 5$  ps (blue line) after the cooling process has ended, the ultimate 1S bleach is not enhanced, but actually decreases relative to the situation without pre-excitation, probably due to the decrease in the ground-state absorption at the time the push arrives (transition to  $X_1$ ). Finally, if  $T$  is further increased, this reduction in the yield of excitons from the push is smaller (due to Auger recombination, which regenerates the ground-state population), but the yield never equals that obtained without 800 nm excitation.

Noteworthy is a red shift of several nanometers of the 1S bleach band after pre-excitation, as shown most clearly in the normalized 1S close-ups in panel B of Figure 4. This is assigned to a progressive enhancement of biexciton (BX) shifting with the number of excitons per particle.<sup>32,33</sup> Since our sample is almost completely excited with at least a single exciton following the 800 nm pulse, the additional excitons

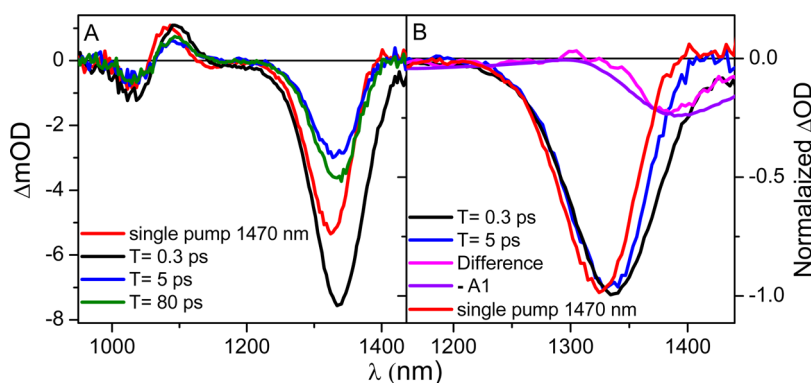


**Figure 4.** (A) Comparison of the band edge bleach induced by 1470 nm excitation without (red) or with “preheating” of the sample with an initial above band gap pulse timed “ $T$ ” ps before the NIR pulse according to diagram A in Scheme 1 with  $\tau = 1$  ps. (B) Normalized difference spectra presented in panel A and the difference between the plots representing  $T = 0.3$  ps and  $T = 5$  ps, compared to the A1 absorption band. For details on how this feature was extracted see the text.

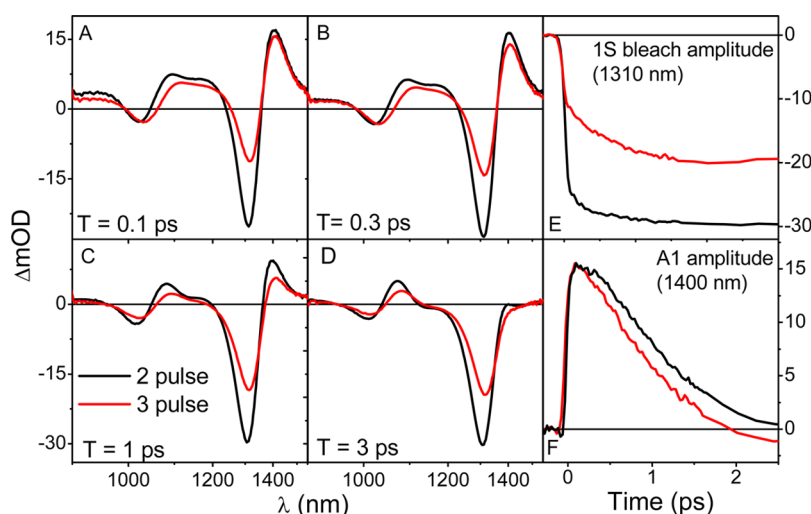


**Figure 5.** Comparison of the spectral and temporal response of the 3.5 nm QD sample to excitation at 650 nm with (red line) or without (black line) initial saturation of the sample with cold single excitons in the particles. Panels A–D present transient spectra for a series of delays  $T$  after the visible excitation pulse as designated in each. Panels E and F present temporal changes observed at the peaks of 1S bleach and of the A1 band, respectively.

generated by the push are producing BX and higher. Panel B also highlights an extra broadening to the red of the bleach at  $T = 300$  fs. Upon subtraction from the blue curve, this difference quantitatively reproduces the A1 band (purple line), indicating that the NIR push has erased this hot induced absorption.

**“Spectator” Effects on Hot Exciton Transient Spectra.** According to spectra in Figure 1, the A1 band is the only spectral range where selective optical pumping of hot exciton states is possible in the presence of pristine QDs. Akin to macroscopic slabs of semiconductor, QD absorption cross sections rise monotonically with photon energy. Once the photon energy is increased sufficiently,  $\sigma(\lambda)$  is nearly unchanged by photoabsorption by a small number of photons.<sup>32,34</sup> Ironically, this situation presents yet another opportunity for applying double-pump–probe methods to QD photo-physics. Insensitivity of absorption cross sections to coexisting excitons allows accurate dosing of additional quanta into the sample regardless of the exciton number state. As shown below, this can be used for testing the linearity of the BE bleach with the number of excitons and for preparing an intriguing biexciton state composed of one hot and one cold e–h pair.

To prepare the latter, the sample is first excited with an intense 800 nm pulse ( $\eta_0(\lambda_{800}) = 1.5$ ), generating a population where a large majority of QDs have absorbed at least one photon. Accordingly the optical density of the sample is adjusted to be relatively thin at the pump wavelength ( $\sim 0.4$ ), ensuring that nearly all QDs are excited even at the back surface of the cell without dangerously high initial photon densities in front. After  $\sim 100$  ps, once multiexcitons have recombined, the sample is made up almost exclusively of cold monoexcitons. Then a second weak push centered at 650 nm ( $\eta_0(\lambda_{650}) = 0.3$ ) impinges on the sample and

generates a population of mixed hot and cold biexcitons. Note that again optical chopping is conducted on the 650 nm pump only so QDs that do not absorb at least one 650 nm photon do not contribute to the  $\Delta\text{OD}$  signal. The results are presented, along with a control experiment in which the 800 nm pump was blocked, in Figure 5. This comparison is quantitative and reflects an identical concentration and distribution of additional excitations introduced by the 650 nm push. Thus, the reduction in the depth of the 1S bleach in all panels when a spectator exciton is present indicates a clear departure from linearity with the exciton number  $N_x$ , already going from one to two excitations. We stress that this bleach feature served as an effective exciton “counter” in numerous studies of multiexciton generation (MEG), based on the assumption of its linearity with  $N_x$ .<sup>35–38</sup>

Besides a mild red shift in the 1S bleach, a quantitative comparison shows that spectator presence reduces the initial amplitude of the 1S bleach to less than 45% of that without prior excitation. Even after the hot excitons cool to the band edge, the bleach amplitude is not restored and remains only around 70% of that without spectators. This growth from 45% to 70% in the bleach amplitude reflects another spectator effect on cooling dynamics. While the bleach amplitude increase during monoexciton cooling is small ( $\leq 15\%$ ), a cold spectator leads to a delayed near doubling of this feature over several picoseconds. Remarkably the initial A1 absorption band intensity is totally unaffected by an additional exciton and decays with identical kinetics that nearly match that of the delayed rise in BE bleach. Finally, the same insensitivity to the presence of spectator excitons is exhibited by the initial 1P bleach as well, once subtracted from the



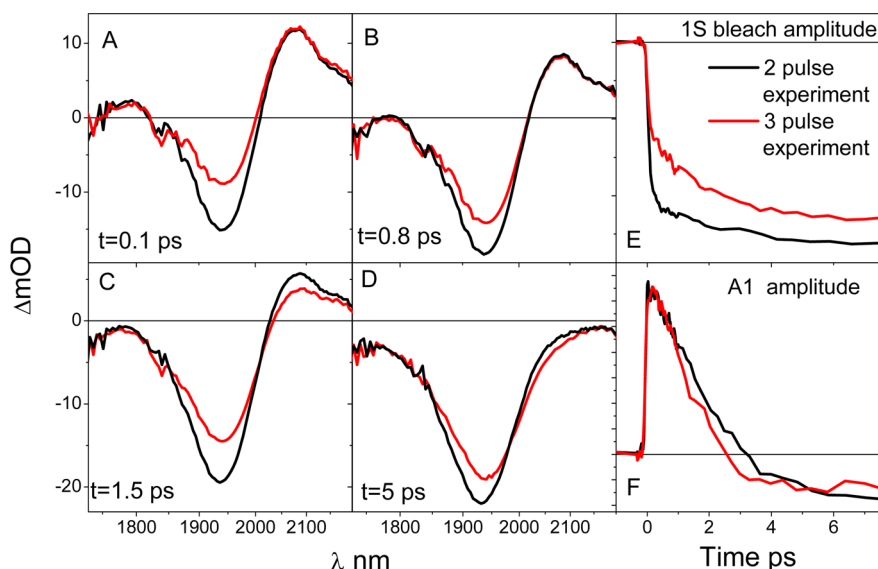


**Figure 6.** Same as Figure 5 for the larger QD sample. In this case excitation pulses were derived from the laser fundamental at 800 nm.

absorptive background. This is in perfect agreement with the kinetic correlation observed between the A1 and 1P features in the  $\Delta\Delta\text{OD}$  measurements from our earlier study.<sup>21</sup>

The same approach was used on the 7 nm sample, producing the results shown in Figure 6. In this case the dosing and spectator generation were both obtained with 800 nm pulses derived from the amplifier fundamental. General trends are conserved showing a reduced depth of 1S bleach and an unaffected A1 band. In the larger sample spectator-induced reduction in bleach amplitude was milder, amounting to  $\sim 80\%$  of the single exciton bleach once cooling is complete. Comparing decay kinetics of spectral features related to the process of exciton cooling shows an identical time scale for A1 band erasure, regardless of the sample size, as demonstrated in panel B of Figure 7. In contrast the delayed rise in 1S bleach, which is prominent in the presence of spectator excitons, is nearly 2 times slower in the larger nanocrystals. This departure suggests that the similarity in these decay rates found for 3.5 nm QDs (as can be seen in panels E and F of Figure 5) is coincidental and that the two signatures probably reflect distinct processes, as found previously for CdSe.<sup>3</sup>

**Pump Intensity Dependence of TA.** The nonlinear growth in the 1S bleach with  $N_x$  contradicts numerous earlier claims, including one global fitting analysis of PbSe TA from this lab.<sup>20</sup> If correct, this sublinear dependence should be easily detectable in an intensity dependence of TA when pumping high above the BG, where the absorption cross section is impervious to the pump fluence. Under such conditions, as long as the probability for completely Fermi blocking all eight degenerate band edge transitions<sup>39</sup> remains negligible, the bleach should grow linearly with fluence. In view of this

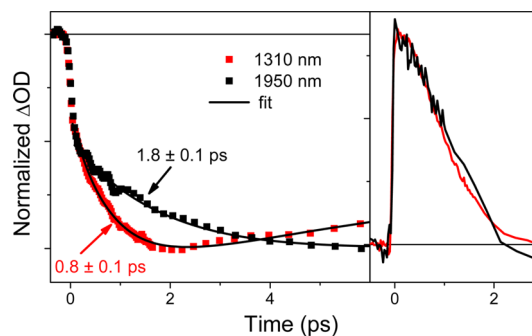


**Figure 7.** Comparison of cooling kinetics in small and large QD samples. Panel A shows delayed rise in the band edge bleach for spectator containing QDs, along with biexponential fits and resulting rise times. Panel B presents a similar decay of the A1 band for the same two samples.

inconsistency, the effect of pump fluence on the BE bleach intensity of 3.5 nm QDs was measured meticulously, producing the data for Figure 8.

At early times two unexpected phenomena are clearly visible: (1) the relative contribution of delayed rise to the BE bleach is significantly enhanced as the fluence is increased. (2) The maximum bleach value (noted as “a” in panel A and B) is not linear with the intensity of the pump for larger fluences, which are all low enough to exclude true saturation of the 8-fold degenerate BE transition. Both the sublinear fluence dependence and the appearance of a two-staged rise in the 1S band are in full agreement with the spectator effects described above, since as the fluence is increased, the contribution of higher and higher multi-excitons, which can be seen as mutual spectators, rises steadily.

After 3 ps the initial rapid stage of evolution associated with the exciton cooling is over, and a gradual decay of the  $\Delta\text{OD}$  signal is observed, leveling off after a

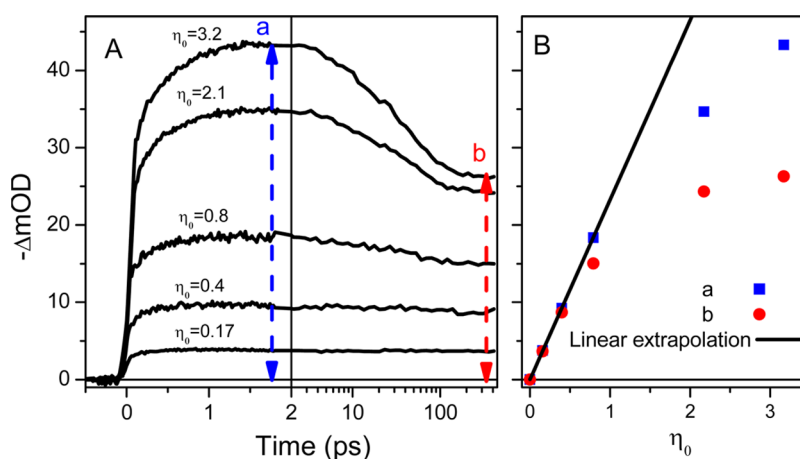


**Figure 8.** (A) Spectral cuts at the band gap after excitation at 650 nm for different pump fluences. (B) Bleach amplitudes at delays “a” and “b” as designated in panel A for the same pump fluences.

delay of  $\sim 100$  ps. This is the anticipated signature of multiple exciton annihilation due to Auger recombination. As expected, the prominence of this stage of evolution is dependent upon the distribution of exciton number states generated. Clearly, at the lowest pump fluence, the induced bleach is essentially constant and free of multiexciton recombination effects. Since the sample is optically thin, the designated values of  $\eta$  are nearly conserved throughout this sample. Finally, following Auger recombination, a long-lived difference spectrum characteristic of singly excited QDs remains, which does not decay significantly in our observation window. All of the observations above support the notion that, contrary to earlier reports, the 1S bleach of excited QDs does not rise linearly as the band edge states are filled and that this departure from linearity is apparent already for the second exciton.

## DISCUSSION

**Short-Time Spectra of Single/Double Hot/Cold Excitons.** Despite the multipulse sequences employed here, the new insights gained in this study are apparent already from the power dependence of the 1S bleach plotted in Figure 8: (A) In PbSe QDs the delayed rise in the 1S-1S bleach assigned to exciton cooling and state filling is strongly enhanced in its relative amplitude for hot multiexcitons. (B) The bleach of the 1S band increases nonlinearly with the average number of excitons per QD, much before significant blocking of the BE transition.

Despite the qualitative agreement of three pulse experiments with trends recorded with fluence-dependent pump–probe, they are not directly comparable. The reason for this is that they lack a common reference. In two-pulse pump–probe one subtracts a transient absorption spectrum at the designated delay after the pump from that obtained without it. In contrast, for three-pulse spectator-effect experiments, the same procedure is repeated for a sample that is first saturated with cold excitons. Thus, none of the four

spectra employed to extract both data sets are the same. In order to put both data sets into quantitative reference, we have subtracted a correctly scaled difference spectrum of a cold monoexciton (MX) from the three-pulse spectra. This allows both data sets to be compared directly, as both are then referenced to absorption of the sample before any excitation. Quantitative extraction of cold monoexciton difference spectra was obtained by characterizing the particle cross section and performing pump–probe experiments at low pump fluence (see details in the Supporting Information).

Such manipulation provides six different  $\Delta\text{OD}$  spectra, which are characteristic of the six possible permutations of two excitons in two QDs, where both excitons can be either hot or cold. The lower panel compares the difference spectrum of a cold BX (gray) with that of two cold MX (pink). Above are equivalent difference spectra for one hot BX (blue), two hot MX (black), a mixed hot plus cold BX (red), and finally one cold and one hot MX (green). Hot and cold BX spectra were extracted by subtraction of single exciton contributions to data at intermediate intensities after careful characterization of the absorption cross sections at 650 nm as described in the Supporting Information. To clarify what these spectra represent, a level scheme of two nanocrystals is presented with Figure 9, where the excitations in the pair of particles are color coded in accordance with the curves in the figure itself. For reference, the green difference spectrum pertaining to one hot plus one cold MX is portrayed in both panels.

**Assignment of the A1 Band.** Numerous studies have associated the A1 band with biexciton shifting of all the remaining band edge electrons.<sup>11,12,40,41</sup> If this is the case, the amplitude of this band and its peak wavelength must be correlated. A simple simulation reveals that the shift needed to generate the observed induced absorption peak is on the order of the width of the transition ( $\sim 60$  meV). That shift is nearly equal to the full width of the 1S transition in the pristine sample,

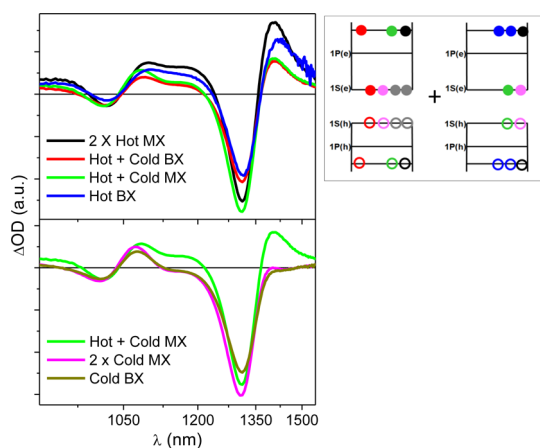


**Figure 9.** Graphical comparison of the six possible characteristic difference spectra for two excitons in two quantum dots, where either of the excitations can be “hot” or “cold”. The legend on the right depicts the distribution and energy content of the excitons producing the correctly colored difference spectrum on the left.

and thus the induced absorption would be nearly as intense as the original 1S band, or nearly 6 times more intense than that observed. This is demonstrated in Figure S2 in the Supporting Information. Clearly the assumption above needs to be re-examined.

The first striking observation from comparing the spectra in Figure 9 is that the amplitude of the A1 band depends nearly linearly on the number of HOT excitons, with no observable dependence on their distribution in the two QDs. Thus, the A1 band in the mixed BX is identical in shape and amplitude to that obtained by the sum of one hot and one cold MX. This is also the case for two hot MX or one hot BX, which overlap for most of the induced absorption band, probably due to the enhanced overlap with 1S bleach due to BX shifting. In contrast, the 1S bleach is strongly affected by the distribution of the excitons, being lower in amplitude once both excitons coexist in a single QD. Notice also that the similarity in the difference spectra of the mixed BX or the sum of one hot and one cold MX is also apparent for the early bleach in the 1P band and in the induced absorption between the two low-lying features.

Insensitivity of the A1 band to the distribution of the hot excitons that generate it strongly suggests it is a hot band due to the excited excitons themselves, *i.e.*, reflects secondary excitation by the probe of one or both of the hot carriers and not of other band edge electrons whose transition energy has been shifted by prior excitation. This goes also for the broad induced absorption spanning the 1S to 1P bands and the initial 1P bleach as well. This assignment agrees also with the observation that secondary excitation in the A1 band not only changes the number of excitons but also erases the A1 band in the absorbing QD. This complete erasure would not be expected if the absorption stemmed from the remaining band edge electrons,

since a significant fraction of them would continue absorbing even after the additional excitation.

This assignment raises the question of how a secondary excitation leads to additional excitons with high probability. In our experimental search for signs of MEG in PbSe, none was observed up to a total photon energy three times that of the band edge.<sup>20</sup> In the current experiments, if all the energy from both excitations is pooled, it should add up to nearly 3 times the band gap. However, in PbSe the light quantum is evenly split between electron and hole, so that the first photon is effectively contributing only half its energy to either. The second potentially deposits another full band gap of energy to one of the two hot carriers, bringing the sum total to that which would be deposited by a single photon 4 times the BG in energy. Whether this is enough to generate a significant MEG yield or whether the two-photon aspect of energy deposition is the key to this efficiency is the subject for future investigation. Excitation with photons containing 4 times the BG energy have been reported to produce non-negligible amounts of impact ionization even in bulk PbSe.<sup>42</sup>

We note in passing that below band edge induced absorptions have in some cases been assigned to sample charging and irreversible damage.<sup>31,43</sup> That absorption, however, was shown to be much longer lived ( $\tau > 100$  ps) and to extend much deeper into the red. In addition, the presence of sample charging here was ruled out by comparing fluence-dependent data with and without sample cell translation, which rapidly refreshed the irradiated volume with no apparent difference in signal strength or temporal variation.

**Nonlinear Bleaching of the 1S Band.** The other significant observation here is the deviation of the 1S band bleach with  $N_x$ . It is clearly demonstrated in Figures 5, 6, 8, and 9 and is upheld also when plotting the band area and not its peak amplitude, excluding the possibility that this trend has to do with broadening and not changes in absorbance. Figure 6 demonstrates that this trend is not sample dependent and has been observed in all our experiments that have addressed this point directly. This finding is at variance with almost all previous reports on PbSe QDs, and there is nothing in the observations themselves to explain its origin. We note that there is one previous theoretical publication that due to carrier–carrier interactions predicts nonlinearity in multiexciton absorption cross sections for CdSe QDs.<sup>44</sup> Another study presented experimental results, but it involved very high excitation intensities and made photophysical assumptions that go against the current wisdom concerning the relevance of stimulated emission to the transient absorption measurements in this material.<sup>45</sup> In any case the nonlinear increase of the BE bleach with the number of excitons, even when relaxed to the band edge, questions the reliance on the single-exciton



bleach to monitor the degeneracy of the intense low-energy transitions. In future experiments we intend to address this by extending the measurements to even higher multiexcitons to obtain its  $N_x$  dependence.

Spectral evolution that accompanies exciton cooling was the subject of an earlier study in our laboratories and demonstrated that it includes several distinct bands that decay on different time scales. Nonetheless, the disappearance of the A1 band and the pronounced buildup of the BE bleach seen very clearly in the data presented in Figure 5 would suggest that both changes take place with similar kinetics and are governed by a single process. It is noteworthy that the experiments reported for the 7 nm sample dispel even this similarity and show that the delayed 1S bleach buildup can be much longer than the A1 decay, which appears not to vary with the particle size. It is possible that these two signatures reflect different dependence on the excess energy of the same carriers or involve different band evolution. Interpreting this will also require further study.

## EXPERIMENTAL METHODS

**PbSe QDs Synthesis.** The PbSe QDs were synthesized using a slight variation of the previously reported procedure.<sup>21</sup> The reaction mixture consisting of 4 mmol of PbO, 12 mmol of oleic acid, and 10 mL of hexadecane (HDC) was heated to 100 °C under vacuum for 1 h. The injection temperature of 90 °C was adjusted under a nitrogen atmosphere. Then the injection of 4 mmol of trioctylphosphine selenide (TOPSe; 2 M) solution into the reaction mixture was immediately followed by the injection of 2 mL of diphenylphosphine (DPP). Then, the temperature was reduced to the growth temperature of 80 °C. The reaction was quenched by addition of acetone, and the QDs were separated by centrifugation. The precipitate was isolated from the supernatant under nitrogen conditions (in a glovebox) and dispersed in hexane, and acetone was added. Then, the supernatant was removed, while the precipitate was dried under a nitrogen atmosphere and finally dissolved in hexane under a nitrogen atmosphere.

**Pump–Probe Experiments.** All samples were handled in oxygen-free environments and irradiated in airtight 1 mm path length optical glass cuvettes at room temperature. The laser system and methods of measurement have been described in detail elsewhere.<sup>46</sup> For the 3.5 nm diameter sample 1  $\mu$ J of the 30 fs output from a homemade multipass amplified titanium sapphire system was focused in 3 mm of sapphire to generate supercontinuum probe pulses from 0.9 to 1.7  $\mu$ m. Another portion of the amplified fundamental was used to generate pump pulses, either directly at  $\sim$ 800 nm or by pumping a TOPAS (light conversion) to produce  $\sim$ 40 fs pump pulses centered at 650 nm and/or 1470 nm. For the larger sized QD sample, probe pulses were derived from the TOPAS idler, covering the range from 1.8 to 2  $\mu$ m. Intensity spectra of the various laser pulses used, as well as the absorption spectra provided the probes' wavelength-dependent group delay and indicated a pump–probe cross-correlation of  $\sim$ 100 fs throughout the probed range. After the sample, the probe pulses were collected with reflective optics into InGaAs photodiode array spectrometers (BTC 261E or BTC 262E, BWTek) alternately with and without sample pumping. Subtraction of these produced the time-dependent difference spectra displayed here, which were corrected for the measured probe group delay.

## CONCLUSIONS

Double pump–probe spectroscopy has been employed to assign the origins of band edge bleach and below band edge induced absorption band that arise in hot exciton states in PbSe QDs. Re-exciting in that below band gap induced absorption is shown to produce additional excitons with high probability. In addition, pump–probe experiments on a sample saturated with single relaxed excitons prove that the resulting  $1S_e1S_h$  bleach is not linear with the number of excitons per nanocrystal. This finding is verified by examining the intensity dependence of two pulse pump–probe experiments in two samples differing significantly in size, demonstrating its generality. Analysis of the results suggests that below band edge induced absorption in hot exciton states is due to excited state absorption and not to shifted absorption of cold carriers and that  $1S_e1S_h$  bleach signals are not an accurate counter of sample excitons when their distribution includes multiexciton states.

*Conflict of Interest:* The authors declare no competing financial interest.

*Supporting Information Available:* Calculation of the absorption cross section for the 3.5 nm PbSe QD and A1 band intensity simulation. This material is available free of charge via the Internet at <http://pubs.acs.org>.

*Acknowledgment.* S.R. acknowledges support from the Israel Science Foundation (ISF) and the US–Israel Binational Science Foundation (BSF). The ISF is administered by the Israel Academy of Sciences and the Humanities. E.L. acknowledges support from the Volkswagen Foundation, the Niedersachsen-Deutsche Technion Gesellschaft, and Focal Area Technology (FTA) from the Council for Higher Education, Israel.

## REFERENCES AND NOTES

- Achermann, M.; Hollingsworth, J. A.; Klimov, V. I. Multiexcitons Confined within a Subexcitonic Volume: Spectroscopic and Dynamical Signatures of Neutral and Charged Biexcitons in Ultrasmall Semiconductor Nanocrystals. *Phys. Rev. B* **2003**, *68*, 245302.
- Prezhdo, O. V. Photoinduced Dynamics in Semiconductor Quantum Dots: Insights from Time-Domain *ab Initio* Studies. *Acc. Chem. Res.* **2009**, *42*, 2005–2016.
- Sewall, S. L.; Cooney, R. R.; Anderson, K. E.; Dias, E. A.; Sagar, D. M.; Kambhampati, P. State-Resolved Studies of Biexcitons and Surface Trapping Dynamics in Semiconductor Quantum Dots. *J. Chem. Phys.* **2008**, *129*, 084701.
- Klimov, V. I.; McBranch, D. W.; Leatherdale, C. A.; Bawendi, M. G. Electron and Hole Relaxation Pathways in Semiconductor Quantum Dots. *Phys. Rev. B* **1999**, *60*, 13740.
- Bockelmann, U. Exciton Relaxation and Radiative Recombination in Semiconductor Quantum Dots. *Phys. Rev. B* **1993**, *48*, 17637.
- Guyot-Sionnest, P.; Shim, M.; Matranga, C.; Hines, M. Intra-band Relaxation in CdSe Quantum Dots. *Phys. Rev. B* **1999**, *60*, 2181–2184.
- Efros, A. L.; Kharchenko, V. A.; Rosen, M. Breaking the Phonon Bottleneck in Nanometer Quantum Dots: Role of Auger-Like Processes. *Solid State Commun.* **1995**, *93*, 281–284.

8. An, J. M.; Califano, M.; Franceschetti, A.; Zunger, A. Excited-State Relaxation in PbSe Quantum Dots. *J. Chem. Phys.* **2008**, *128*, 164720.
9. Wang, W.; Califano, M.; Zunger, A. Pseudopotential Theory of Auger Processes in CdSe Quantum Dots. *Phys. Rev. Lett.* **2003**, *91*, 056404.
10. Klimov, V. I. Spectral and Dynamical Properties of Multiexcitons in Semiconductor Nanocrystals. *Annu. Rev. Phys. Chem.* **2007**, *58*, 635–673.
11. Kambhampati, P. Hot Exciton Relaxation Dynamics in Semiconductor Quantum Dots: Radiationless Transitions on the Nanoscale. *J. Phys. Chem. C* **2011**, *115*, 22089–22109.
12. Klimov, V. I. Optical Nonlinearities and Ultrafast Carrier Dynamics in Semiconductor Nanocrystals. *J. Phys. Chem. B* **2000**, *104*, 6112–6123.
13. Cooney, R. R.; Sewall, S. L.; Dias, E. A.; Sagar, D. M.; Anderson, K. E.; Kambhampati, P. Unified Picture of Electron and Hole Relaxation Pathways in Semiconductor Quantum Dots. *Phys. Rev. B* **2007**, *75*, 245311.
14. Kambhampati, P. Unraveling the Structure and Dynamics of Excitons in Semiconductor Quantum Dots. *Acc. Chem. Res.* **2010**, *44*, 1–13.
15. Burda, C.; Link, S.; Green, T. C.; El-Sayed, M. A. New Transient Absorption Observed in the Spectrum of Colloidal CdSe Nanoparticles Pumped with High-Power Femtosecond Pulses. *J. Phys. Chem. B* **1999**, *103*, 10775–10780.
16. Schins, J. M.; Trinh, M. T.; Houtepen, A. J.; Siebbeles, L. D. Probing Formally Forbidden Optical Transitions in PbSe Nanocrystals by Time- and Energy-Resolved Transient Absorption Spectroscopy. *Phys. Rev. B* **2009**, *80*, 035323.
17. Nozik, A. J. Spectroscopy and Hot Electron Relaxation Dynamics in Semiconductor Quantum Wells and Quantum Dots. *Annu. Rev. Phys. Chem.* **2001**, *52*, 193–231.
18. Harbold, J.; Du, H.; Krauss, T.; Cho, K.-S.; Murray, C.; Wise, F. Time-Resolved Intraband Relaxation of Strongly Confined Electrons and Holes in Colloidal PbSe Nanocrystals. *Phys. Rev. B* **2005**, *72*, 195312.
19. Trinh, M. T.; Sfeir, M. Y.; Choi, J. J.; Owen, J. S.; Zhu, X. A Hot Electron–Hole Pair Breaks the Symmetry of a Semiconductor Quantum Dot. *Nano Lett.* **2013**, *13*, 6091–6097.
20. Gdor, I.; Sachs, H.; Roitblat, A.; Strasfeld, D. B.; Bawendi, M. G.; Ruhman, S. Exploring Exciton Relaxation and Multiexciton Generation in PbSe Nanocrystals Using Hyperspectral Near-IR Probing. *ACS Nano* **2012**, *6*, 3269–3277.
21. Gdor, I.; Yang, C.; Yanover, D.; Sachs, H.; Lifshitz, E.; Ruhman, S. Novel Spectral Decay Dynamics of Hot Excitons in PbSe Nanocrystals: A Tunable Femtosecond Pump–Hyperspectral Probe Study. *J. Phys. Chem. C* **2013**, *117*, 26342–26350.
22. Liljeroth, P.; van Emmichoven, P. A. Z.; Hickey, S. G.; Weller, H.; Grandidier, B.; Allan, G.; Vanmaekelbergh, D. Density of States Measured by Scanning-Tunneling Spectroscopy Sheds New Light on the Optical Transitions in PbSe Nanocrystals. *Phys. Rev. Lett.* **2005**, *95*, 086801.
23. Trinh, M. T.; Houtepen, A. J.; Schins, J. M.; Piris, J.; Siebbeles, L. D. A. Nature of the Second Optical Transition in PbSe Nanocrystals. *Nano Lett.* **2008**, *8*, 2112–2117.
24. Peterson, J. J.; Huang, L.; Delerue, C.; Allan, G.; Krauss, T. D. Uncovering Forbidden Optical Transitions in PbSe Nanocrystals. *Nano Lett.* **2007**, *7*, 3827–3831.
25. Wehrenberg, B. L.; Wang, C.; Guyot-Sionnest, P. Interband and Intraband Optical Studies of PbSe Colloidal Quantum Dots. *J. Phys. Chem. B* **2002**, *106*, 10634–10640.
26. Ruhman, S.; Hou, B.; Friedman, N.; Ottolenghi, M.; Sheves, M. Following Evolution of Bacteriorhodopsin in Its Reactive Excited State via Stimulated Emission Pumping. *J. Am. Chem. Soc.* **2002**, *124*, 8854–8858.
27. Kraack, J. P.; Wand, A.; Backup, T.; Motzkus, M.; Ruhman, S. Mapping Multidimensional Excited State Dynamics Using Pump-Impulsive-Vibrational-Spectroscopy and Pump-Degenerate-Four-Wave-Mixing. *Phys. Chem. Chem. Phys.* **2013**, *15*, 14487–14501.
28. Bismuth, O.; Komm, P.; Friedman, N.; Eliash, T.; Sheves, M.; Ruhman, S. Deciphering Excited State Evolution in Halorhodopsin with Stimulated Emission Pumping. *J. Phys. Chem. B* **2010**, *114*, 3046–3051.
29. Nirmal, M.; Murray, C. B.; Bawendi, M. G. Fluorescence-Line Narrowing in CdSe Quantum Dots: Surface Localization of the Photogenerated Exciton. *Phys. Rev. B* **1994**, *50*, 2293.
30. Bawendi, M. G.; Carroll, P. J.; Wilson, W. L.; Brus, L. E. Luminescence Properties of CdSe Quantum Crystallites: Resonance between Interior and Surface Localized States. *J. Phys. Chem.* **1992**, *96*, 946–954.
31. Tyagi, P.; Kambhampati, P. False Multiple Exciton Recombination and Multiple Exciton Generation Signals in Semiconductor Quantum Dots Arise from Surface Charge Trapping. *J. Chem. Phys.* **2011**, *134*, 094706.
32. Geiregat, P.; Houtepen, A.; Justo, Y.; Grozema, F. C.; Van Thourhout, D.; Hens, Z. Coulomb Shifts upon Exciton Addition to Photoexcited PbS Colloidal Quantum Dots. *J. Phys. Chem. C* **2014**, *118*, 22284–22290.
33. Kambhampati, P. Multiexcitons in Semiconductor Nanocrystals: A Platform for Optoelectronics at High Carrier Concentration. *J. Phys. Chem. Lett.* **2012**, *3*, 1182–1190.
34. Cho, B.; Peters, W. K.; Hill, R. J.; Courtney, T. L.; Jonas, D. M. Bulklike Hot Carrier Dynamics in Lead Sulfide Quantum Dots. *Nano Lett.* **2010**, *10*, 2498–2505.
35. Ellingson, R. J.; Beard, M. C.; Johnson, J. C.; Yu, P.; Micic, O. I.; Nozik, A. J.; Shabaev, A.; Efros, A. L. Highly Efficient Multiple Exciton Generation in Colloidal PbSe and PbS Quantum Dots. *Nano Lett.* **2005**, *5*, 865–871.
36. Nozik, A. J. Multiple Exciton Generation in Semiconductor Quantum Dots. *Chem. Phys. Lett.* **2008**, *457*, 3–11.
37. Padilha, L. A.; Stewart, J. T.; Sandberg, R. L.; Bae, W. K.; Koh, W. K.; Pietryga, J. M.; Klimov, V. I. Carrier Multiplication in Semiconductor Nanocrystals: Influence of Size, Shape, and Composition. *Acc. Chem. Res.* **2013**, *46*, 1261–1269.
38. Trinh, M. T.; Houtepen, A. J.; Schins, J. M.; Hanrath, T.; Piris, J.; Knulst, W.; Goossens, A.; Siebbeles, L. D. In Spite of Recent Doubts Carrier Multiplication Does Occur in PbSe Nanocrystals. *Nano Lett.* **2008**, *8*, 1713–1718.
39. Kang, I.; Wise, F. W. Electronic Structure and Optical Properties of PbS and PbSe Quantum Dots. *J. Opt. Soc. Am. B* **1997**, *14*, 1632.
40. Gao, Y.; Talgorn, E.; Aerts, M.; Trinh, M. T.; Schins, J. M.; Houtepen, A. J.; Siebbeles, L. D. Enhanced Hot-Carrier Cooling and Ultrafast Spectral Diffusion in Strongly Coupled PbSe Quantum-Dot Solids. *Nano Lett.* **2011**, *11*, 5471–5476.
41. Nootz, G.; Padilha, L. A.; Levina, L.; Sukhovatkin, V.; Webster, S.; Brzozowski, L.; Sargent, E. H.; Hagan, D. J.; Van Stryland, E. W. Size Dependence of Carrier Dynamics and Carrier Multiplication in PbS Quantum Dots. *Phys. Rev. B* **2011**, *83*, 155302.
42. Pijpers, J. J. H.; Ulbricht, R.; Tielrooij, K. J.; Osherov, A.; Golan, Y.; Delerue, C.; Allan, G.; Bonn, M. Assessment of Carrier-Multiplication Efficiency in Bulk PbSe and PbS. *Nat. Phys.* **2009**, *5*, 811–814.
43. Kambhampati, P. On the Kinetics and Thermodynamics of Excitons at the Surface of Semiconductor Nanocrystals: Are There Surface Excitons?. *Chem. Phys.* **2015**, *446*, 92–107.
44. Franceschetti, A.; Zhang, Y. Multiexciton Absorption and Multiple Exciton Generation in CdSe Quantum Dots. *Phys. Rev. Lett.* **2008**, *100*, 136805.
45. Lenngren, N.; Garting, T.; Zheng, K.; Abdellah, M.; Lascoux, N.; Ma, F.; Yartsev, A.; Zidek, K.; Pullerits, T. Multiexciton Absorption Cross Sections of CdSe Quantum Dots Determined by Ultrafast Spectroscopy. *J. Phys. Chem. Lett.* **2013**, *4*, 3330–3336.
46. Wand, A.; Rozin, R.; Eliash, T.; Jung, K. H.; Sheves, M.; Ruhman, S. Asymmetric Toggling of a Natural Photoswitch: Ultrafast Spectroscopy of Anabaena Sensory Rhodopsin. *J. Am. Chem. Soc.* **2011**, *133*, 20922–20932.